

# Calculation of the exchange constants of the Heisenberg model in the plane-wave based methods using the Green's function approach

Dm.M. Korotin,<sup>1</sup> V.V. Mazurenko,<sup>2</sup> V.I. Anisimov,<sup>1,2</sup> and S.V. Streltsov<sup>1,2</sup>

<sup>1</sup>*Institute of Metal Physics, S.Kovalevskoy St. 18, 620990 Yekaterinburg, Russia\**

<sup>2</sup>*Ural Federal University, Mira St. 19, 620002 Yekaterinburg, Russia*

(Dated: December 7, 2024)

The approach, which allows to compute exchange parameters of the Heisenberg model in the plane-wave based methods of the band structure calculations is presented. This calculation scheme is based on the Green's function method and Wannier function projection technique. It was implemented in the framework of the pseudopotential method and tested on such materials as NiO and KCuF<sub>3</sub>. Obtained exchange interaction values are in a very good agreement both with results of the total energy calculations and experimental estimations. Presented approach provides an unique way of the analysis of the magnetic interactions, since it allows to calculate different orbital contributions to the total exchange coupling.

## I. INTRODUCTION

Magnetic properties of different materials is one of the most actively studied topics in the modern condensed matter physics. Localized magnetic moments of the system can be described within the Heisenberg model with isotropic exchange interaction

$$H_{Heis} = \sum_{\langle ij \rangle} J_{ij} \hat{\mathbf{S}}_i \hat{\mathbf{S}}_j \quad (1)$$

or its extensions, which take into account symmetric and antisymmetric parts of the anisotropic exchange coupling [1–3]. Therefore one of the most important theoretical problem is how to calculate exchange constants  $J_{ij}$  and do this with a minimal information about the system, i.e. from the “first principles”.

One of the most popular approaches for the *ab initio* investigation of the solids is the density functional theory (DFT). There are few methods how to estimate exchange constants  $J$  within the DFT, i.e. how to map the results of the DFT calculations onto the Heisenberg model.

The most direct, and most popular way is in the calculation of the total energies of the  $N + 1$  magnetic configurations, where  $N$  is the number of different exchange constants  $J_{ij}$  [4–6]. The approach being robust has several serious drawbacks: (1) quite a number of different magnetic configurations has to be calculated for complicated systems; (2) in each configuration one needs to keep magnetic moments the same (important for the materials close to itinerant regime); and (3) the result is just a number, which is hard to analyze, i.e. understand which orbitals mostly contribute and what is the mechanism of the exchange coupling (direct exchange, super-exchange, double exchange etc.).

These shortcomings can be overcome in the Green's function method [7–9], which is based on finding of analytical expressions for the changes of the total energy in

the DFT calculation and Heisenberg model with respect to small spin rotations. This approach allows not only to get all exchange constants in the calculations of a *single* magnetic configuration, but also to find contributions coming from different orbitals (i.e., e.g.  $J_{xy/xy}$ ,  $J_{xy/x^2-y^2}$  etc.) to the total exchange. Moreover, this method can be easily generalized to calculate anisotropic part of the exchange hamiltonian [10].

The Green's function approach was formulated for the methods, which deals with localized orbitals, as e.g. the linear muffin-tin orbitals (LMTO) method [11] or linear combination of atomic orbitals (LCAO) [12, 13]. However, modern high-precision schemes of the band structure calculations are mostly based on the methods, which have plane-wave part of the wave-function (these are the full-potential (linearized) augmented plane-wave (L)APW [14] and pseudopotential [5] methods). As a result a straightforward realization of the Green's function methods becomes impossible within plane-waves approaches and all its advantages cannot be used in the modern *ab initio* DFT codes without direct definition of localized basis set.

In the present paper we show how the Green's function approach could be adapted for the plane-wave based methods using Wannier functions formalism. We implemented this calculation scheme in the pseudopotential Quantum-ESPRESSO code [15] and present the results for two transition metal compounds: NiO and KCuF<sub>3</sub>.

## II. METHOD

Following Ref. [8] we used classical analogue of Eq. (1) with spins substituted by the unit vectors  $\mathbf{e}_i$  pointing in the direction of the  $i$ th site magnetization:

$$H = \sum_{\langle ij \rangle} J_{ij} \mathbf{e}_i \mathbf{e}_j. \quad (2)$$

The value of the exchange constants for the conventional classical Heisenberg model (with spins, not unit vectors) can be obtained with a proper renormalization.

---

\*Electronic address: dmitry@korotin.name

The essence of the Green's function method is in the application of the local force theorem (see e.g. Ref. [16]) to the change of the spin density in the DFT due to rotation of the spins on a small angle  $\delta\phi$  [8]. This can be done if the Hamiltonian of the system is defined in the localized orbitals basis set (otherwise it is not clear what parts of the Hamiltonian have to be rotated). The result of the rotation is compared with a similar procedure performed for the spin Hamiltonian (2), which allows to get an analytical expression for the exchange integrals (8). The major difficulty in the application of this approach to the modern plane-wave based calculation schemes is the absence of the localized basis set in these methods. We propose to use the Wannier functions (WF) projection procedure to avoid this restriction and show its realization for the pseudopotential method.

Wannier functions are the most general and natural choice for description of localized correlated electronic states. The localization degree and the symmetry of such wavefunctions could be controlled in the projection procedure. One of the most widespread procedure is an enforcement of maximum localization of WF [17]. The second one [18] is a constraint of the WF symmetry to be the same as the symmetry of pure atomic  $d$ -orbitals.

In the present paper the second type of projection procedure is used. WFs were generated as projections of the pseudoatomic orbitals  $|\phi_{n\mathbf{k}}\rangle = \sum_{\mathbf{T}} e^{i\mathbf{k}\cdot\mathbf{T}} |\phi_n^{\mathbf{T}}\rangle$  onto a subspace of the Bloch functions  $|\Psi_{\mu\mathbf{k}}\rangle$  (the detailed description of WFs construction procedure within pseudopotential method is given in Ref. [19]):

$$|W_n^{\mathbf{T}}\rangle = \frac{1}{\sqrt{N_{\mathbf{k}}}} \sum_{\mathbf{k}} |W_{n\mathbf{k}}\rangle e^{-i\mathbf{k}\cdot\mathbf{T}}, \quad (3)$$

where

$$|W_{n\mathbf{k}}\rangle \equiv \sum_{\mu=N_1}^{N_2} |\Psi_{\mu\mathbf{k}}\rangle \langle \Psi_{\mu\mathbf{k}} | \phi_{n\mathbf{k}} \rangle. \quad (4)$$

Here  $\mathbf{T}$  is the lattice translation vector. The resulting WFs have symmetry of the atomic orbitals  $\phi_n$  and describe electronic states that form energy bands numbered from  $N_1$  to  $N_2$ .

The matrix elements of the one-electron Hamiltonian in reciprocal space are defined as:

$$H_{nm,\sigma}^{WF}(\mathbf{k}) = \langle W_{n\mathbf{k}} | \left( \sum_{\mu=N_1}^{N_2} |\Psi_{\mu\mathbf{k}}\rangle \varepsilon_{\mu}^{\sigma}(\mathbf{k}) \langle \Psi_{\mu\mathbf{k}} | \right) | W_{m\mathbf{k}} \rangle, \quad (5)$$

where  $\varepsilon_{\mu}^{\sigma}(\mathbf{k})$  is the eigenvalue of the one-electron Hamiltonian for band  $\mu$  and spin  $\sigma$ .

Such a Hamiltonian matrix is produced as a result of the WF projection procedure at the end of the self-consistent cycle in the spin-polarized DFT or DFT+U approach.

This matrix being rearrange in the  $H_{mm',ij,\sigma}^{WF}$  form (where  $m$  and  $m'$  numerate orbitals on  $i$ th and  $j$ th sites

respectively) can be used for the inter-sites Green's function calculation at every  $\mathbf{k}$ -point in reciprocal space:

$$G_{ij,\sigma}^{mm'}(\varepsilon, \mathbf{k}) = (\varepsilon + E_F - H_{mm',ij,\sigma}^{WF}(\mathbf{k}))^{-1}, \quad (6)$$

where  $E_F$  is the Fermi energy. The site indexes  $i$  and  $j$  run through atoms within primitive cell by default, however the inter-site Green's function between any two atoms of the lattice sites  $i'$  and  $j'$  could be obtained via integration over Brillouin zone (BZ):

$$G_{i'j',\sigma}^{mm'}(\varepsilon) = \int_{BZ} G_{ij,\sigma}^{mm'}(\varepsilon, \mathbf{k}) e^{i\mathbf{k}(\mathbf{R}_{i'} - \mathbf{R}_i) - (\mathbf{R}_{j'} - \mathbf{R}_j)} d\mathbf{k}, \quad (7)$$

where  $G_{ij,\sigma}^{mm'}(\mathbf{k})$  is the inter-site Green's function of the primitive cell for given  $\mathbf{k}$  point,  $\mathbf{R}_{i'}$  – position of atom  $i'$  in the lattice and  $\mathbf{R}_i$  position of the same atom within the primitive cell.

Resulting  $G_{i'j',\sigma}^{mm'}(\varepsilon)$  is used in the analytic expression for the exchange integrals as obtained in the Green's function method [8]:

$$J_{ij} = -\frac{1}{2\pi} \int_{-\infty}^{E_F} d\varepsilon \sum_{\substack{m''m''' \\ m''m'''}} \text{Im}(\Delta_i^{mm'} G_{ij,\downarrow}^{m''m'''} \Delta_j^{m''m'''} G_{ji,\uparrow}^{m''m'''}), \quad (8)$$

where  $G_{ji,\uparrow}^{mm'}$  ( $G_{ij,\downarrow}^{mm'}$ ) is real-space inter-site Green's function for spin up (down) obtained in Eq. (7) and

$$\Delta_i^{mm'} = \int_{BZ} (H_{ii,\uparrow}^{mm'}(\mathbf{k}) - H_{ii,\downarrow}^{mm'}(\mathbf{k})) d\mathbf{k}. \quad (9)$$

This scheme allows to compute per-orbital contribution to the exchange interaction between two atoms. Without spin-orbit coupling the  $\Delta_i^{mm'}$  matrix is diagonal in the spin subspace, but it is not necessarily diagonal in the orbital subspace. However, one may always transform  $\Delta_i^{mm'}$  to the diagonal form (e.g. changing global coordinate system to the local one, when axes are directed to the ligands; or simply diagonalizing on-site Hamiltonian matrix in the WF basis set):

$$\Delta_i^{mm'} = \sum_{\mathbf{k}} T_i^{mk} \tilde{\Delta}_i^{kk} (T_i^{km'})^*. \quad (10)$$

Then Eq. (8) can be rewritten as:

$$J_{ij}^{kk'} = -\frac{1}{2\pi} \int_{-\infty}^{E_F} d\varepsilon \sum_{kk'} \text{Im}(\tilde{\Delta}_i^{kk} \tilde{G}_{ij,\downarrow}^{kk'} \tilde{\Delta}_j^{k'k'} \tilde{G}_{ji,\uparrow}^{k'k}), \quad (11)$$

where

$$\tilde{G}_{ij,\sigma}^{kk'} = \sum_{mm'} T_i^{km} \tilde{G}_{ij,\sigma}^{mm'} (T_j^{m'k'})^*. \quad (12)$$

Eq. (11) allows to calculate exchange coupling between  $k$ th orbital on site  $i$  and  $k'$ th orbital on site  $j$ .

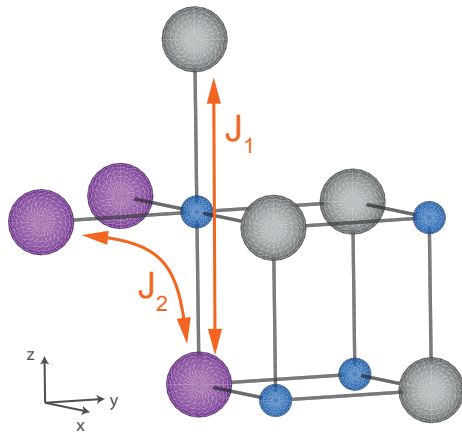


Figure 1: (color online) Schematic view of the NiO crystal structure. Blue spheres denote oxygen ions, gray and magenta spheres denote two magnetic types on Ni ions. The figure was drawn using VESTA [20] software.

### III. RESULTS AND DISCUSSION

#### A. NiO

NiO is one of the typical objects on which different calculation schemes are tested. It is a charge-transfer insulator with the band gap  $\sim 4$  eV [21] and local magnetic moment  $1.77\mu_B$  [22]. NiO crystallizes in the rock-salt (NaCl) structure and exhibits an antiferromagnetic ordering of type-II fcc (AFM II-type) [23], with planes of opposite spins being repeated in alternating order along [111], see Fig. 1. This type of magnetic ordering is due to the strong next-nearest-neighbor (nnn) coupling between nickel ions via oxygens  $2p$  shell. The Néel temperature is  $T_N=523\text{K}$  [24].

Since an account of the strong electronic correlations is crucial in the case of NiO [25], we used the LSDA+U method [26] for the calculation of electronic and magnetic properties. On-site Coulomb repulsion and intra-atomic Hund's rule exchange parameters were chosen to be  $U = 8.0$  eV and  $J_H = 0.9$  eV respectively [25]. We used Perdew-Zunger version of the exchange-correlation potential [27], 45 Ry and 360 Ry for the charge density and kinetic energy cut-offs, and 512  $\mathbf{k}$  points in the Brillouin-zone for integration in the course of the self-consistency. The unit cell consists of two formula units to simulate AFM II-type.

First of all, we have calculated dominating exchange between second nearest neighbors interaction,  $J_1$  (see Fig. 1), using conventional total energy technique and have obtained that  $J_1 = 18.8$  meV, which perfectly agrees with experimental estimation of  $J_1 = 19.0$  meV [28].

The small effective Hamiltonian used for the Green's function calculation according to (6) was obtained by the Wannier function projection procedure as described in Sec. II. The Wannier functions were constructed as a projection of Ni  $3d$  and O  $2p$  pseudoatomic orbitals

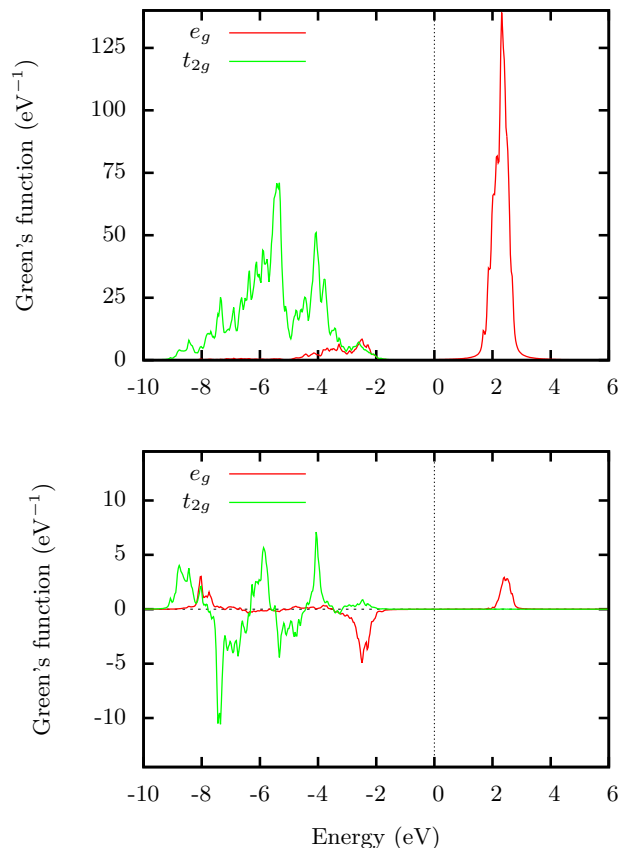


Figure 2: (color online) Imaginary part of spin-up on-site (upper panel) Green's function of Ni ion and inter-site (lower panel) Green's function for the pair of the Ni ions along  $c$  axis (i.e. corresponding to  $J_1$ ). Green's function for  $e_g$  states is shown by solid red line, for  $t_{2g}$  states by the solid green one. Zero energy corresponds to the Fermi level.

onto subspace of Bloch functions defined by the 32 energy bands, which predominantly have the Ni  $3d$  and O  $2p$  character (2 formula units  $\times$  2 spins  $\times$  (5 Ni  $3d$  plus 3 O  $2p$  orbitals)=32).

The exchange constants calculated by the Green's function method equal  $J_1 = 18.9$  meV,  $J_2 = -0.4$  meV, which agrees both with the total energy and experimental estimations. Moreover, it allows to perform analysis of the partial contributions coming from different orbitals. Orbital resolved matrix (in meV) for the largest exchange interaction  $J_1$  between next nearest neighbors (calculated according to (11)) is given below

$$J_1^{mm'} = \begin{pmatrix} -18.9 & 0 & 0 & 0 & 0 \\ 0.0 & 0 & 0 & 0 & 0 \\ 0.0 & 0 & 0 & 0 & 0 \\ 0.0 & 0 & 0 & 0 & 0 \\ 0.0 & 0 & 0 & 0 & 0 \end{pmatrix}, \quad (13)$$

where the following order of the  $3d$ -orbital is used:  $3z^2 - r^2$ ,  $zx$ ,  $zy$ ,  $x^2 - y^2$ ,  $xy$  and axis of the coordinate system are shown in Fig. 1. Thus, one may see that

the exchange coupling between next nearest neighbors is due to overlap between  $3z^2 - r^2$  orbitals centered on different sites. This is the  $180^\circ$  superexchange interaction via  $2p_z$  orbital of the oxygen sitting between two Ni ions in the  $z$  ( $c$ ) direction, which has to be strong and antiferromagnetic (AFM) according to Goodenough-Kanamori-Anderson rules [29]. In contrast, exchange interaction between nearest neighbors,  $J_2$ , occurs via two orthogonal  $p$  orbitals and is expected to be weak and ferromagnetic (FM) [29].

An imaginary part of on-site and inter-site Green's functions are shown in Fig. 2. The inter-site Green's function (lower panel) corresponds to the strongest  $180^\circ$  exchange coupling,  $J_1$ . The exchange interaction (8) is the energy integral of two Green's functions and two  $\Delta$ -functions, which do not depend on  $\epsilon$ . Therefore it is important to explore an energy dependence of the Green's function.

One can see that on-site Green's function (upper panel) doesn't change its sign for all energy interval and after normalization the function exactly equals to density of electronic states. The energy integral of the on-site Green's function up to the Fermi level results in the total number of electrons on corresponding orbitals. This value is predictable and a slight changes in the on-site Green's function peaks positions and widths will not change resulted number of electrons significantly.

The inter-site Green's function, shown on the lower panel of Fig. 2 changes the sign several times. It means that in general case the energy integral up to the Fermi level has unpredictable sign and the value that strongly depends on the Green's function peaks position and widths, i.e. on bands structure calculation results.

### B. $\text{KCuF}_3$

$\text{KCuF}_3$  is renowned due to the orbital order, which defines its magnetic properties. The single hole in the  $e_g$  subshell of  $\text{Cu}^{2+}$  ion (electronic configuration is  $3d^9$ ) is localized on the alternating in the  $ab$  plane  $z^2 - x^2$  and  $z^2 - y^2$  orbitals (i.e. antiferro-orbital order), which results in the weak ferromagnetic coupling in this plane. In contrast, there is a ferro-orbital ordering in the  $c$  direction, which leads to the strong antiferromagnetic interaction along this axis. As a result in the essentially three dimensional (3D) crystal one may observe formation of nearly ideal one-dimensional antiferromagnetic Heisenberg chains [30, 31].

The compound has a distorted cubic perovskite crystal structure (shown on Fig. 3) with space group  $I4/mcm$ . The copper ions have octahedral fluorine surrounding. These octahedra are elongated along one of the directions. At room temperature, there are two different structural polytypes with antiferro ( $a$ -type) and ferrolike ( $d$ -type) stacking of the  $ab$  planes along the  $c$  axis.[32]

Altogether, the electronic and structural properties of  $\text{KCuF}_3$  have been intensively studied so far employ-

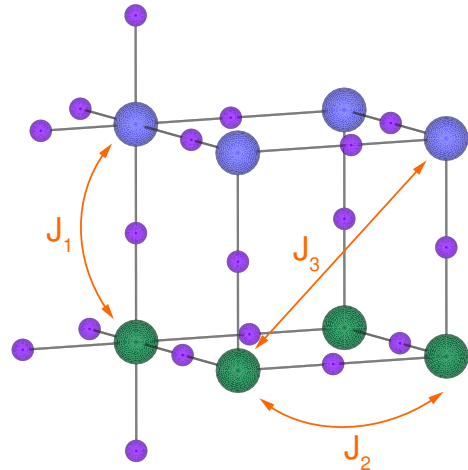


Figure 3: (color online) Schematic view of the  $\text{KCuF}_3$  crystal structure. Blue and green spheres denote Cu ions of two different types, violet spheres denote F ions, potassium ion in the center of the cell is not shown for clearness.

ing density functional theory and its extensions like the DFT+U approach [33]. The DFT+U calculations give the correct insulating ground state with the correct spin and orbital ordering [34–36]. We took the GGA+U approach as a starting point for the exchange interaction parameters calculation.

For the density-functional calculations, we used the Perdew–Burke–Ernzerhof [37] GGA exchange–correlation functional together with Vanderbilt ultrasoft pseudopotentials. We set the kinetic energy cutoff equals 50 Ry (400 Ry) for the plane-wave expansion of the electronic states (core-augmentation charge). The self-consistent calculation was performed with the  $4 \times 4 \times 4$  Monkhorst–Pack  $k$ -point grid. We set the effective on-site Coulomb interaction  $U_{eff} = U - J_H = 6.6$  eV [36]. To reproduce magnetic and orbital ordering of the polytype  $a$  in the compound we used a cell containing four formula units.

The basis of the WFs had a dimension equal 56. It included 20 Cu- $d$  like WFs (5 functions for every Cu site) and 36 F- $p$  like WF. We generated the Cu WF using a linear combination of atomic Cu- $d$  orbitals to obtain more clear physical basis for Green's function.

The strongest exchange interaction was found to be between nearest Cu ions along the  $c$  axis,  $J_1 = 17$  meV (antiferromagnetic). As it was mentioned above this is because of the ferro-orbital order in this direction,  $J_1 \sim t^2/U$ . Calculated value agrees with different experimental estimations of  $J_1$ , which was found be 16.1 meV [38] using analysis of the specific heat data, 16.2 meV [39] basing on the temperature dependence of the magnetic susceptibility, 17 meV[40] or 17.5 meV [41] in neutron measurements.

The exchange coupling in the  $ab$  plane has to be much weaker,  $J_2 \sim t^2 J_H/U^2$ , since there is antiferro-orbital order. Our calculations give  $J_2 = 0.5$  meV. And an ad-

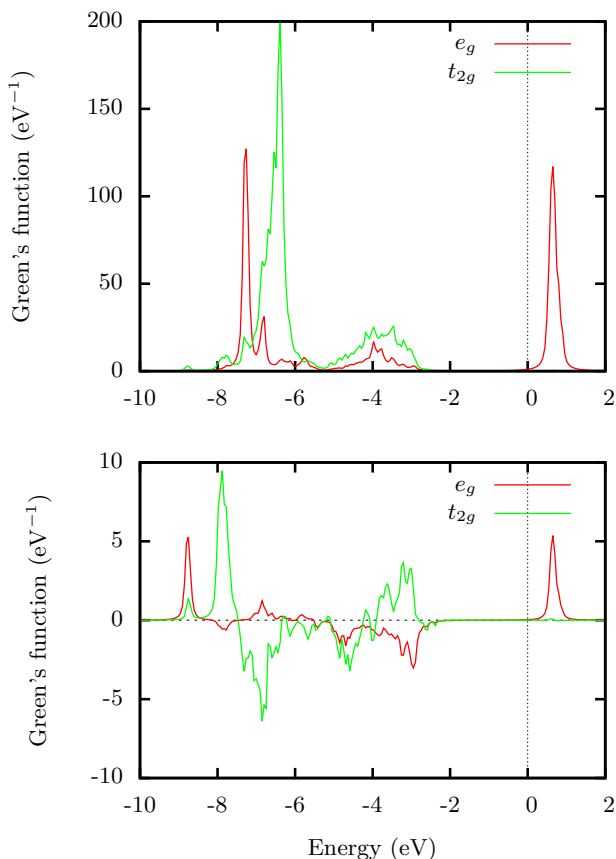


Figure 4: (color online) Imaginary part of spin-down on-site (upper panel) Green's function of Cu ion and inter-site (lower panel) Green's function for two Cu ions corresponding to  $J_1$ . Green's function for  $e_g$  states is shown by solid red line, for  $t_{2g}$  states by the solid green one. Zero energy corresponds to the Fermi level.

ditional “diagonal” exchange  $J_3$  was estimated to be -1 meV.

The on-site and inter-site Green's functions for  $\text{KCuF}_3$  are shown in Fig. 4. The main contribution to exchange interaction in  $c$  direction comes from the overlap between  $z^2 - y^2$  WFs centered on different Cu ions.

#### IV. CONCLUSION

We have presented the implementation of the Green's function approach for the Heisenberg model exchange parameters calculation. The localized electronic states are described by the Wannier functions with the symmetry of atomic orbitals. This basis set allows to overcome the limitations of modern plane-wave based calculation schemes and perform complex analysis of the inter-site exchange interaction in the density functional theory or in its extensions such in DFT+U. The results were tested on two transition metal compounds:  $\text{NiO}$  and  $\text{KCuF}_3$ . Obtained values are in excellent agreement with experimental estimations.

#### V. ACKNOWLEDGMENTS

The present work was supported by the grant of the Russian Scientific Foundation (project no. 14-22-00004).

- 
- [1] D. Zakharov, H.-A. von Nidda, M. Eremin, J. Deisenhofer, R. Eremina, and A. Loidl, in *Quantum Magnetism*, edited by B. Barbara, Y. Imry, G. Sawatzky, and P. Stamp (Springer Netherlands, 2008), NATO Science for Peace and Security Series, pp. 193–238, ISBN 978-1-4020-8511-6, URL [http://dx.doi.org/10.1007/978-1-4020-8512-3\\_14](http://dx.doi.org/10.1007/978-1-4020-8512-3_14).
  - [2] S. Blundell, *Magnetism in Condensed Matter*, Oxford Master Series in Condensed Matter Physics (OUP Oxford, 2001), ISBN 9780198505914, URL <http://books.google.ru/books?id=a10tngEACAAJ>.
  - [3] D. Khomskii, *Transition Metal Compounds* (Cambridge University Press, 2014), ISBN 9781107020177, URL <http://books.google.ru/books?id=hEelBAAQBAJ>.
  - [4] L. Noodleman, The Journal of Chemical Physics **74**, 5737 (1981), ISSN 00219606, URL <http://scitation.aip.org/content/aip/journal/jcp/74/10/10.1063/1.340939>.
  - [5] R. M. Martin, *Electronic Structure: Basic Theory and Practical Methods* (Cambridge University Press, 2004), ISBN 9780521782852.
  - [6] A. A. Tsirlin, Physical Review B **89**, 014405 (2014), ISSN 1098-0121.
  - [7] A. Liechtenstein, V. Gubanov, M. Katsnelson, and V. Anisimov, Journal of Magnetism and Magnetic Materials **36**, 125 (1983).
  - [8] A. I. Liechtenstein, M. I. Katsnelson, V. P. Antropov, and V. A. Gubanov, Journal of Magnetism and Magnetic Materials **67**, 65 (1987), ISSN 0304-8853.
  - [9] M. I. Katsnelson and A. I. Lichtenstein, Physical Review B **61**, 8906 (2000), ISSN 0163-1829.
  - [10] V. Mazurenko and V. Anisimov, Physical Review B **71**, 184434 (2005), 0410767v1.
  - [11] O. K. Andersen and O. Jepsen, Physical Review Letters **53**, 2571 (1984).
  - [12] F. Bloch, Zeitschrift für Physik **52**, 555 (1929), ISSN 0044-3328.
  - [13] W. A. Harrison, *Elementary Electronic Structure* (World Scientific, 1999).
  - [14] D. Singh, *Plane waves, pseudopotentials and the LAPW method* (Kluwer Academic, 1994).
  - [15] P. Giannozzi, S. Baroni, N. Bonini, M. Calandra, R. Car, C. Cavazzoni, D. Ceresoli, G. L. Chiarotti, M. Cococ-



- cioni, I. Dabo, et al., *Journal of Physics: Condensed Matter* **21**, 395502 (2009).
- [16] M. Methfessel and J. Kubler, *Journal of Physics F: Metal Physics* **12**, 141 (1982).
- [17] I. Souza, N. Marzari, and D. Vanderbilt, *Physical Review B* **65**, 13 (2001), ISSN 0163-1829.
- [18] V. I. Anisimov, D. E. Kondakov, A. V. Kozhevnikov, I. A. Nekrasov, Z. V. Pchelkina, J. W. Allen, S.-K. Mo, H.-D. Kim, P. Metcalf, S. Suga, et al., *Physical Review B* **71** (2005), ISSN 1098-0121.
- [19] D. Korotin, A. V. Kozhevnikov, S. L. Skornyakov, I. Leonov, N. Binggeli, V. I. Anisimov, and G. Trimarchi, *The European Physical Journal B* **65**, 91 (2008), ISSN 1434-6028.
- [20] K. Momma and F. Izumi, *Journal of Applied Crystallography* **44**, 1272 (2011), ISSN 0021-8898.
- [21] S. Hüfner, J. Osterwalder, T. Riesterer, and F. Hüliger, *Solid State Communications* **52**, 793 (1984), ISSN 00381098.
- [22] B. E. F. Fender, A. J. Jacobson, and F. A. Wedgwood, *The Journal of Chemical Physics* **48** (1968).
- [23] C. G. Shull, W. A. Strauser, and E. O. Wollan, *Phys. Rev.* **83**, 333 (1951).
- [24] J. R. Tomlinson, L. Domash, R. G. Hay, and C. W. Montgomery, *Journal of the American Chemical Society* **77**, 909 (1955).
- [25] V. I. Anisimov, J. Zaanen, and O. K. Andersen, *Physical Review B* **44**, 943 (1991).
- [26] V. I. Anisimov, F. Aryasetiawan, and A. I. Lichtenstein, *J. Phys.: Condens. Matter* **9**, 767 (1997).
- [27] J. P. Perdew and A. Zunger, *Physical Review B* **23**, 5048 (1981), ISSN 0163-1829.
- [28] M. Hutchings and E. Samuelsen, *Phys. Rev. B* **6**, 3447 (1972).
- [29] J. B. Goodenough, *Magnetism and the Chemical Bond* (Interscience publishers, New York-London, 1963).
- [30] K. I. Kugel and D. I. Khomskii, *Soviet Physics Uspekhi* **25**, 231 (1982), ISSN 0042-1294.
- [31] K. Kugel and D. Khomskii, *JETP* **37**, 725 (1973).
- [32] A. Okazaki, *Journal of the Physical Society of Japan* **26**, 870 (1969), ISSN 0031-9015.
- [33] V. I. Anisimov, J. Zaanen, and O. K. Andersen, *Physical Review B* **44**, 943 (1991), ISSN 0163-1829.
- [34] A. I. Liechtenstein, V. I. Anisimov, and J. Zaanen, *Physical Review B* **52**, R5467 (1995), ISSN 0163-1829.
- [35] J. Medvedeva, M. Korotin, V. Anisimov, and A. Freeman, *Physical Review B* **65**, 4 (2002), ISSN 0163-1829.
- [36] N. Binggeli and M. Altarelli, *Physical Review B* **70**, 10 (2004), ISSN 1098-0121.
- [37] J. P. Perdew, K. Burke, and M. Ernzerhof, *Phys. Rev. Lett.* **77**, 3865 (1996), ISSN 1079-7114.
- [38] K. Iio, H. Hyodo, K. Nagata, and I. Yamada, *Journal of the Physical Society of Japan* **44**, 1393 (1978), ISSN 0031-9015.
- [39] S. Kadota, I. Yamada, S. Yoneyama, and K. Hirakawa, *Journal of the Physical Society of Japan* **23**, 751 (1967), ISSN 0031-9015.
- [40] M. T. Hutchings, J. M. Milne, and H. Ikeda, *Journal of Physics C: Solid State Physics* **12**, L739 (1979), ISSN 0022-3719.
- [41] S. Satija, J. Axe, and G. Shirane, *Physical Review B* **21**, 2001 (1980).